Eur Biophys J (2009) 39:121–127
DOI 10.1007/s00249-009-0445-x

ORIGINAL PAPER

Effect of lipid on the conformation of the N-terminal region of equinatoxin II: a synchrotron radiation circular dichroism spectroscopic study

Alison Drechsler · Andrew J. Miles · Raymond S. Norton · B. A. Wallace · Frances Separovic

Received: 27 January 2009 / Revised: 12 March 2009 / Accepted: 16 March 2009 / Published online: 3 April 2009

Abstract Equinatoxin II (EqtII) is a protein toxin that lyses both red blood cells and artificial membranes. Lysis is dependent on the lipid composition, with small unilamellar vesicles (SUVs) of dimyristoylphosphatidylcholine (DMPC) and sphingomyelin (SM) (1:1 molar) being lysed more readily than those of phosphatidylcholine alone. Removing the N-terminus of EqtII prevents pore formation, but does not prevent membrane binding. A peptide corresponding to residues 1–32 of EqtII was found using NMR to adopt a helical structure in micelles. To further understand the structural changes that accompany membrane insertion, synchrotron radiation circular dichroism spectra of the N-terminal peptide in a range of model membranes have been analysed. The peptide structure was examined in water, dodecylphosphocholine (DPC) and DPC:SM (5:1) micelles, and SUVs composed of dioleoylphosphatidylcholine (DOPC) or DMPC, together with SM and cholesterol (Chol). The peptide adopted different conformations in different lipids. Although the presence of SM did not affect the conformation in micelles, inclusion of SM in the bilayer-forming lipid increased the helicity of the peptide. This effect was abolished when Chol was added in DOPC but not in DMPC, which may relate to liquid ordered versus disordered phase properties of the lipid. SM may act as a promoter of membrane organisation necessary for membrane lysis by EqtII.

Keywords Cytolysin · Synchrotron radiation circular dichroism (SRCD) spectroscopy · Secondary structure · Protein–lipid interactions · Equinatoxin II

Abbreviations

Chol	Cholesterol
DMPC	Dimyristoylphosphatidylcholine
DOPC	Dioleoylphosphatidylcholine
DPC	Dodecylphosphocholine
EqtII	Equinatoxin II
LUV	Large unilamellar vesicles
MLV	Multilamellar vesicles
SM	Sphingomyelin
SRCD	Synchrotron radiation circular dichroism
SUVs	Small unilamellar vesicles

Introduction

Equinatoxin II (EqtII) is a member of the actinoporin family of sea anemone toxins, which are highly basic proteins of approximately 20 kDa with lytic activity depending on the presence of sphingomyelin (SM). EqtII

Alison Drechsler and Andrew J. Miles contributed equally to this work.

"Proteins, membranes and cells: the structure–function nexus". Contributions from the annual scientific meeting (including a special symposium in honour of Professor Alex Hope of Flinders University, South Australia) of the Australian Society for Biophysics held in Canberra, ACT, Australia, September 28–October 1, 2008.

A. Drechsler · F. Separovic (✉)
School of Chemistry, Bio21 Institute, University of Melbourne, Melbourne, VIC 3010, Australia
e-mail: fs@unimelb.edu.au

A. J. Miles · B. A. Wallace
Department of Crystallography, Birkbeck College, University of London, London WC1E 7HX, UK

R. S. Norton
The Walter and Eliza Hall Institute of Medical Research, 1G Royal Parade, Parkville, VIC 3052, Australia

lyses both red blood cells and artificial membranes via a multistep pathway, which includes membrane binding, oligomerization and pore formation (Hong et al. 2002). Progression along this pathway is dependent on the lipid composition of the target membrane, with small unilamellar vesicles (SUVs) of dimyristoylphosphatidylcholine (DMPC) and SM (1:1 molar) being lysed more readily than those of phosphatidylcholine alone (Belmonte et al. 1993). During membrane binding, the N-terminal region dissociates from the body of EqtII (Anderluh et al. 1999; Malovrh et al. 2003), interacts with the membrane (Gutiérrez-Aguirre et al. 2004) and then penetrates into, but not through, the lipid bilayer (Malovrh et al. 2003). Residues 10–28 of the N-terminus are amphiphilic, and may form an α-helix with one side interacting with the membrane and the other exposed to solvent, whilst the positively charged residues, Lys30, Arg31 and Lys32, may assist in orienting the toxin. Truncating the N-terminal region reduced the lytic activity of EqtII (Anderluh et al. 1997).

To determine the role of the N-terminus, a peptide composed of residues 1–32 of EqtII was synthesised and its structure determined using NMR in phospholipid micelles (Drechsler et al. 2006). The peptide in dodecylphosphocholine (DPC) micelles was found to be helical from residues 6–28, longer than the 11-residue helix spanning residues 15–26 in the native protein (Athanasiadis et al. 2001; Hinds et al. 2002). The peptide, however, did not appear to insert into the micelle but rather to interact with the lipid surface. Despite the increase in α-helicity and interaction with DPC, the peptide does not show significant lytic activity. The structure of this peptide in lipid bilayers or vesicles has not been reported.

To further understand the nature of the interaction of the peptide with lipids, and provide insight into the mechanism of lysis and the structural changes that accompany membrane insertion, synchrotron radiation circular dichroism (SRCD) spectroscopy has been used to characterise the structure of the N-terminal peptide in a range of model membranes. SRCD spectroscopy is able to produce spectral data that are significantly improved over those obtained using conventional CD instruments for several reasons: (1) SRCD beamlines have a detector geometry that reduces apparent light scattering (Mao and Wallace 1984), which can be problematic for membrane samples, (2) it has a higher sensitivity which allows the use of smaller amounts of protein, and hence the use of higher lipid:peptide ratios, critical for these types of studies, and (3) the data obtained at lower wavelengths (~175 nm compared with 190 nm) can provide more accurate information on secondary structures (Wallace et al. 2003).

Initially, the secondary structure of the peptide in DPC micelles calculated from the SRCD spectra was compared with the structure determined by NMR. The peptide was also examined in water, DPC:SM (5:1) micelles, and SUVs composed of dioleoylphosphatidylcholine (DOPC) or DMPC, together with SM and cholesterol (Chol). Similar studies have been carried out with intact EqtII (Miles et al. 2008), but only small changes in protein conformation were seen as a function of lipid composition. However, in this study, we have focused on a peptide corresponding to the N-terminus of EqtII, where more extensive changes are likely to occur as this region of the protein is expected to undergo more significant changes as a function of lipid composition (Gutiérrez-Aguirre et al. 2004).

Materials and methods

Materials

The N-terminal peptide of EqtII, $EqtII_{1–32}$, was synthesised using solid-phase synthesis by Mimotopes (Melbourne, Australia) and exhibited the expected molecular mass of 3,257 Da by MALDI-TOF mass spectrometry. The peptide (>90% purity) was used without further purification. The sequence is shown below.

SADVAGAVIDGASLSFDILKTVLEALGNVKRK.

Dodecylphosphocholine, dioleoylphosphatidylcholine, dimyristoylphosphatidylcholine and brain SM from Avanti Polar Lipids (Alabaster, USA) and cholesterol from Sigma (St Louis, USA) were used without further purification.

Sample preparation

For micelle studies, a stock solution of DPC dissolved in water (2.4 mg/mL, 5.7 mM) was then divided in two, to be used for the sample and baseline spectra. $EqtII_{1–32}$ peptide was added as described for the SUVs samples.

For the SUVs studies, and the DPC:SM (5:1) sample, the lipids were dissolved in 25% methanol/75% chloroform (v/v) then combined at the appropriate ratio. Solvents were removed by rotary evaporation to produce a lipid film, which was then dried using a high vacuum pump overnight. Lipid films were re-solubilised in MilliQ water and vortexed with glass beads to produce multilamellar vesicles (MLV). Prior to SRCD acquisition, approximately 800 μL of MLV dispersions was sonicated on ice for 30 min, with a 20 s on/off cycle, to produce a translucent solution, representative of SUVs (Cornell et al. 1982). Lipid samples were mixed with 50 μL peptide stock solution (6.5 mg/mL). The pH values of the solutions were adjusted to 7.0 using NaOH or HCl. The samples were centrifuged at ~6,000*g* for 2 min to remove any large vesicles and then de-gassed for 15 min to remove any dissolved oxygen that would absorb in the vacuum ultraviolet region of the spectra. Sample concentrations were 0.3 and ~4 mg/mL

for EqtII$_{1–32}$ and the lipids, respectively, yielding peptide:lipid ratios of 1:60 (mol/mol).

SRCD spectroscopy

Synchrotron radiation circular dichroism spectra were acquired on the SRS Daresbury Laboratories (CD12 beamline) (Clarke and Jones 2004) in a Suprasil quartz circular demountable cell (Hellma UK, Ltd), with a 0.02 cm path length. Typically, spectra were acquired at 25°C, between 280 and 175 nm with an interval of 1.0 nm, and an averaging time of 1 s, unless otherwise specified. At CD12, the SRCD data become unreliable when the HT signal is >600 mV. Therefore, this value was used to determine the low wavelength data cut-off limit. Three repeats of each sample and baseline spectrum were acquired. The instrument was calibrated at the beginning of each beam injection using camphor sulphonic acid (CSA), as described previously (Miles et al. 2003). SUVs stability was verified by comparison of the baseline SRCD and high tension (HT) spectra (the latter being a type of pseudo-absorption spectrum) obtained both before and after sample acquisition, with changes in these spectra suggesting vesicle instability or aggregation.

Analysis of SRCD data

Synchrotron radiation circular dichroism spectra were processed using CDtool software (Lees et al. 2004). Baseline spectra were averaged and then subtracted from the averaged sample spectra. The resulting spectra were zeroed between 263 and 270 nm and smoothed with a Savitsky–Golay filter. A mean residue weight of 101.8 was used in the calculations. The error bars on the plots represent one standard deviation in the repeated measurements.

The secondary structure was calculated from processed SRCD spectra using DICHROWEB (Whitmore and Wallace 2004; Lobley et al. 2002) with the CDSSTR (Compton and Johnson 1986; Manavalan and Johnson 1987), CONTINLL (Provencher and Glockner 1981; Van Stokkum et al. 1990) and SELCON3 (Sreerama and Woody 1993; Sreerama et al. 1999) algorithms and reference set SP175 (truncated) (Lees et al. 2006), which consists of 71 protein spectra; data were analysed between 190 and 260 nm. The uncertainty (±) values reported are 1 standard deviation between the results from all the algorithms. The normalised root mean square deviation (NRMSD) (Brahms and Brahms 1980; Mao and Wallace 1984), which is a reflection of the difference between the experimentally derived values for the mean residue ellipticity and those calculated by the fitting algorithm, was calculated through DICHROWEB, using the equation,

$$\mathrm{NRMSD} = \left[\left(\Sigma_N\left(\theta_{\mathrm{exptl}} - \theta_{\mathrm{calcd}}\right)^2\right) / \left(\Sigma_N \theta^2_{\mathrm{exptl}}\right)\right]^{1/2}$$

where θ_{exptl} and θ_{calcd} are the experimental and calculated mean residue ellipticity, respectively, and N is the number of data points used.

If the NMRSD values obtained during the analysis were exceptionally high or (following normalisation to mean elliptical helicity) the magnitude of a spectrum was obviously wrong (for example, an α-helical spectrum with a magnitude similar to that of the spectrum of a β-sheet protein), it was assumed that material had been lost during the vesicle preparation procedure and that the peptide concentration was inaccurate. In such cases, spectra were scaled using the scaling features in DICHROWEB and CDTool until the NMRSD was minimised, a technique shown previously to produce accurate analyses (Miles et al. 2005).

Results

SRCD spectra of the N-terminal peptide in DPC micelles and water

Synchrotron radiation circular dichroism spectra of EqtII$_{1–32}$ in DPC were acquired at a peptide:lipid ratio of 1:60 (Fig. 1), as used for the NMR structure determination (Drechsler et al. 2006). The SRCD spectra of EqtII$_{1–32}$, however, were acquired at a lower temperature (25°C) than the NMR spectra (45°C) because of experimental limitations. To assess if this had any effect on the structure, conventional CD spectra of the peptide in DPC micelles were compared over the temperature range of 5–65°C (data not shown). These indicated that the peptide structure was stable over this temperature range, with only a slight change in spectra around 65°C, so any differences between the NMR and SRCD compositions could not be attributed to this difference in conditions.

The SRCD spectra of EqtII$_{1–32}$ in DPC and DPC:SM (5:1) were very similar. By comparison, the spectrum of the peptide in water was generally much lower in intensity relative to that in micelles, and the ratio of the 190/208 nm peaks was also lower, suggesting the peptide was less structured in water than in the micelles.

The average secondary structures of EqtII$_{1–32}$, based on SRCD spectra, were calculated using the CONTINLL, SELCON3 and CDSSTR algorithms and reference set SP175 (truncated); the results are shown in Table 1. The secondary structure in DPC:SM (5:1), with 35 (±1)% helix, and 19 (±2)% strand, was similar to that in DPC (39 (±2)% helix and 15 (±2)% strand). In water, the helical

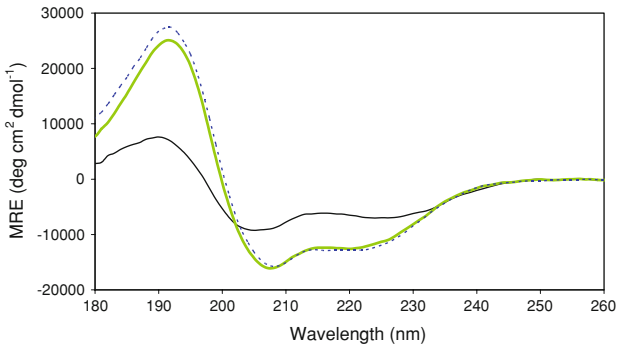

Fig. 1 SRCD spectra of the N-terminal peptide in H_2O (*black solid line*), DPC (*green solid line*), or DPC:SM (5:1) (*blue dashed line*), at a peptide:lipid ratio of 1:60, pH 7, and 25°C in a 0.02 cm cell

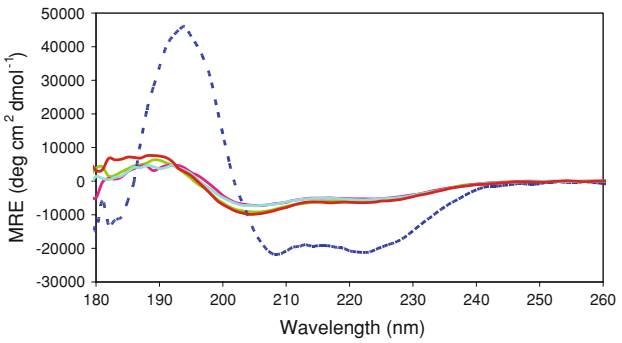

Fig. 2 SRCD spectra of the N-terminal peptide in SUVs of DOPC (*green solid line*), DOPC:SM (1:1) (*dark blue dashed line*), DOPC:Chol (2:1) (*red solid line*), DOPC:SM:Chol (1:1:1) (*purple solid line*), and DOPC:SM:Chol (8:1:1) (*light blue solid line*), at peptide:lipid (1:60), pH 7, 25°C in 0.02 cm cell

Table 1 Secondary structure of the N-terminal peptide in different lipid compositions, calculated in DICHROWEB using the CONTINLL, SELCON3 and CDSSTR algorithms and reference set SP175 (truncated)

Lipids	Percentage of helix	Percentage of strand
H_2O	21 (±0)	22 (±3)
DPC	39 (±2)	15 (±2)
DPC:SM (5:1)	35 (±1)	19 (±2)
DOPC	17 (±1)	20 (±2)
DOPC:SM (1:1)	67 (±7)	3 (±1)
DOPC:SM:Chol (1:1:1)	18 (±1)	26 (±3)
DOPC:SM:Chol (8:1:1)	17 (±1)	27 (±3)
DOPC:Chol (2:1)	17 (±1)	27 (±1)
DMPC	23 (±1)	23 (±1)
DMPC:SM (1:1)	48 (±1)	18 (±1)
DMPC:SM:Chol (1:1:1)	47 (±3)	11 (±2)

content was considerably lower (21 (±0)%), consistent with the diminished 190/208 peak ratio.

Peptide in DOPC, SM and Chol bilayers

Synchrotron radiation circular dichroism spectra of EqtII$_{1–32}$ in DOPC, SM and Chol SUVs are shown in Fig. 2. Spectra in all DOPC systems except the DOPC:SM mixture were similar, with only a slight variation in the intensity of the absorbance minima. The spectrum in the DOPC:SM mixture was of much higher magnitude and had a much higher 190/208 ratio, both of which indicate that the peptide is much more helical in this environment.

The calculated percentages of secondary structure of EqtII$_{1–32}$ in DOPC and mixed DOPC SUVs are shown in Table 1. The fractions of helix in DOPC, DOPC:Chol, DOPC:SM:Chol (1:1:1) and DOPC:SM:Chol (8:1:1) were similar, ~17 (±1)%, although the peptide in DOPC alone contained less β-strand (18% compared with ~27%). However, the peptide had a high-helical content (67%) in DOPC:SM, again consistent with the appearance of the spectra. These results suggest that, in DOPC, the structure is less helical than in DPC, which has 26 (±2)% helix. However, in contrast to our observations with DPC samples, inclusion of SM in DOPC caused a dramatic increase in helicity.

Peptide in DMPC, SM and Chol bilayers

Synchrotron radiation circular dichroism spectra of EqtII$_{1–32}$ in DMPC SUVs of different compositions are shown in Fig. 3. The SUVs produced from DMPC with Chol were unstable, so no spectra were acquired for either DMPC:Chol (2:1) or DMPC:SM:Chol (8:1:1) compositions. These SUVs were probably less stable at 25°C because of a higher gel-fluid phase transition temperature of 23°C for DMPC compared with below 0°C for DOPC (Marsh 1990). The DMPC:Chol (2:1) and DMPC:SM:Chol (8:1:1) bilayers are in the vicinity of the phase transition temperature, where SUVs are less stable than when in the more fluid phase (Cornell et al. 1981; Cornell et al. 1982). SM promotes liquid-ordered/liquid-disordered phase separation in model membranes (Schön et al. 2008), and the SUVs high in SM, DMPC:SM (1:1) and DMPC:SM:Chol (1:1:1), are more stable.

Synchrotron radiation circular dichroism spectra of the N-terminal peptide were different in each of the DMPC compositions (Fig. 3). As shown in Table 1, the secondary structure of the peptide in DMPC was 23 (±1)% helix and 23 (±1)% strand. There was a significant increase in helical content in DMPC:SM:Chol (1:1:1), with 47 (±3)% helix and 11 (±2)% strand, and in DMPC:SM (1:1) with 48 (±1)% helix and 18 (±1)% strand. Thus, as in DOPC, the inclusion of SM tended to increase the peptide helical structure in DMPC, but, unlike in DOPC, the presence of Chol did not inhibit that increase.

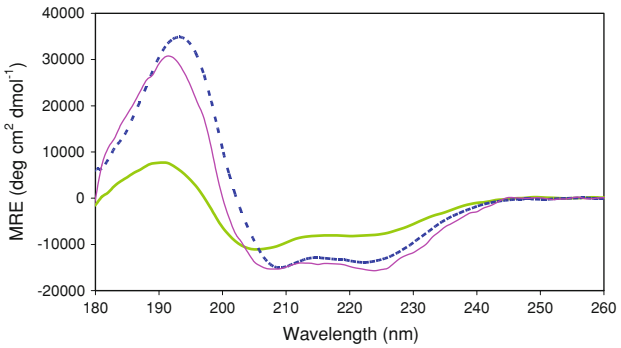

Fig. 3 SRCD spectra of the N-terminal peptide in SUVs (peptide:lipid 1:60) composed of DMPC (*green solid line*), DMPC:SM (1:1) (*blue dashed line*), and DMPC:SM:Chol (1:1:1) (*purple solid line*), pH 7, 25°C, 0.02 cm cell

Discussion

Equinatoxin $II_{1–32}$ peptide in water was shown to be largely unordered by both NMR (Drechsler et al. 2006) and SRCD (this study). This result was not unexpected as peptides that are not constrained by disulphide bonds are often very flexible and do not adopt regular secondary structures in aqueous solution.

Our SRCD study of $EqtII_{1–32}$ in a range of lipid systems was carried out at a 60:1 molar ratio of lipid-to-peptide. Although peptide structure and lipid phase are known to be dependent on concentration (Cornell et al. 1988), this concentration was chosen for comparison with the peptide structure in DPC micelles as determined by NMR (Drechsler et al. 2006). Despite this, the fraction of the residues that are in a helical conformation in the NMR structure differs significantly from the SRCD experiments in DPC (68 vs. 39%), respectively. The difference cannot be attributed to different temperatures used for data collection, because a conventional CD study of this sample as a function of temperature showed that the results were essentially independent of the temperature of the experiment. The differences may relate to the CD reference database used, which is based on the structures of globular aqueous protein structures, whereas the N-terminus of EqtII may more closely resemble a membrane-based peptide, for which there are at present no suitable reference databases (Whitmore and Wallace 2008). However, the most likely source of the discrepancy between the structures is that the CD results are a simple average of all conformations present in the solution, including the bound and free peptide structures and ordered and disordered forms, whereas the NMR results would favour the bound (structured) conformations because of the dependence of NOE-based distance restraints on the inverse sixth power of the distance. Thus, shorter distances in the bound conformation dominate the observed average NOEs. The helical content inferred from the NMR study reflects the fraction of the peptide that is helical when bound to micelles, whereas the helical content inferred from SRCD reflects the average of free and bound states. If we were to assume that the helical content in water (21% helical) reflects the "free" state and that the NMR structure (68% helical) reflects the "bound" state, then we could estimate that the 39% helical content seen in the DPC samples indicates that $\sim$1/3 of the peptide is bound to the micelles. However, this calculation assumes that all of the peptide in water is in a single conformation, whereas it is more likely that the water "conformation" is actually an unknown mixture of conformations with different helical contents.

The shapes of the SRCD spectra of $EqtII_{1–32}$ in all lipid samples examined here showed similar absorbance maxima ($\sim$195 nm) and minima ($\sim$205 and 225 nm), but the intensities of these absorbances, the ratios of the 190/208 nm peaks, and the exact peak wavelengths were dependent on lipid. The peptide conformation may also depend on the order or fluidity of the different lipid systems. The lipid acyl chains of the DPC micelles are less ordered than those of the bilayer-forming lipids in the SUVs, and the DMPC bilayer is more ordered than the DOPC bilayer at 25°C. Cholesterol promotes lipid segregation into DOPC-enriched, liquid-disordered, and SM-enriched, liquid-ordered phases (Kahya et al. 2003). Coexistence of liquid-disordered and liquid-ordered phases is seen in giant unilamellar vesicles for DOPC:SM:Chol (1:1:1), but not for the other DOPC compositions studied here, which are in the liquid-disordered phase at this temperature. The DMPC:SM (1:1) and DMPC:SM:Chol, however, are in the liquid-ordered state (Filippov et al. 2003).

In the micellar environment, the presence of SM had little effect, but in both the lipid bilayers SM on its own increased the helical content considerably. The helical content seen in DOPC:SM is 67%, nearly identical to that calculated from the structure determined by NMR for the peptide in DPC micelles, and it is tempting to speculate that in this lipid mixture, the equilibrium conformation is shifted almost entirely to the ordered state that is detected in the NMR experiments. Interestingly, this is the most ordered DOPC mixed lipid system (Kahya et al. 2003). There is no consistent pattern in the presence of Chol, with all DOPC samples containing cholesterol having minimal ordering (i.e. similar secondary structure to the peptide in aqueous solution), but in the DMPC:SM mixture Chol had little effect on the peptide structure. The DOPC:SM bilayers with cholesterol are in a liquid-disordered phase (Kahya et al. 2003), whereas the DMPC bilayers with cholesterol are in the liquid-ordered phase.

The peptide is more structured in SUVs containing 50% SM, with DOPC:SM (1:1) having the most helical structure

followed by DMPC:SM (1:1). The helical content is almost 50% in the more ordered bilayers DMPC:SM (1:1) and DMPC:SM:Chol (1:1), where the lipid is in the liquid-ordered phase. The peptide had a lower helical content (17%) in DOPC SUVs, where the lipid would be in a liquid-disordered phase, than in water (21%), and a slightly higher helical content (23%) in DMPC SUVs. It appears that the order of the lipid chains is affecting the peptide conformation, with less helix in the more disordered, longer chain lipid and more in the more ordered, shorter chain DMPC SUVs. However, in micelles, the peptide may be adopting a surface conformation as reported by NMR, which would favour an amphipathic helical structure and result in the higher helical content (39% in DPC and 35% in DPC:SM (5:1) micelles). In contrast, in the less highly curved SUVs, the peptide may be partially inserting into the lipid bilayer. Similar behaviour is seen for melittin, which adopts a surface conformation in micelles but inserts into vesicle bilayers (Smith et al. 1994).

Equinatoxin II has a specific interaction with SM, with the highest lytic activity towards membranes containing 50% SM (Belmonte et al. 1993). SRCD studies of full-length EqtII in these lipid systems detected only very small differences in the overall protein structure when SM was present (Miles et al. 2008), with the only significant changes detected in DOPC lipids. In this study we focused on $EqtII_{1–32}$, where any structural changes in the N-terminus of EqtII would be easier to distinguish, as the interacting residues would represent a higher proportion of the total structure.

Overall, the helical content was higher under all conditions suggesting that the N-terminal peptide is more helical than the rest of the protein. SM also had different effects on the peptide in the different lipid systems, with the largest change in DOPC followed by DMPC. Chol in DOPC vesicles reduced the helical content to less than in water, but it did not affect the helical content in DMPC:SM (1:1) SUVs. These structural differences may be related to lipid properties, with the shorter chain, saturated DMPC being less fluid than the longer chain, DOPC vesicles. The α-helical structure is presumably necessary but not sufficient to induce lysis as the peptide does not cause dye leakage in DMPC:SM or DOPC:SM vesicles (Drechsler et al. 2006).

Fluorescence experiments using giant unilamellar vesicles (Schön et al. 2008) show that EqtII binds preferentially to the liquid-ordered rather than liquid-disordered phase and tends to concentrate at domain boundaries. Although SM strongly enhances membrane binding, EqtII formed pores in giant unilamellar vesicles containing SM only when liquid-ordered and disordered phases co-existed. Our SRCD results demonstrate the importance of lipid in determining the peptide structure, with the more fluid or disordered lipid vesicles supporting lower helical contents and the less fluid or more ordered bilayers, DOPC:SM and DMPC:SM, promoting the greatest increase in α-helix. Since the ability of the N-terminal region of EqtII to dissociate from the rest of the protein and associate with the target membrane is necessary for EqtII activity (Hong et al. 2002) and the conformation of $EqtII_{1–32}$ is lipid-dependent, our results are consistent with a dual role of SM as a specific receptor for EqtII and as a promoter of the membrane organisation necessary for membrane lysis.

Acknowledgments Supported by grants from the BBSRC to BAW, Australian Research Council to FS, and by a beamtime grant from the CCLRC to FS and a CCLRC joint programme mode access grant to BAW and R.W. Janes (Queen Mary, Univ. of London). RSN is supported by a fellowship from the Australian National Health and Medical Research Council. We wish to thank Dr Gregor Anderluh for useful discussions.

References

Anderluh G, Pungerčar J, Križaj I, Strukelj B, Gubenšek F, Maček P (1997) N-Terminal truncation mutagenesis of equinatoxin II, a pore-forming protein from the sea anemone *Actinia equina*. Protein Eng 10:751–755. doi:10.1093/protein/10.7.751

Anderluh G, Barlič A, Podlesek Z, Maček P, Pungerčar J, Gubenšek F, Zecchini ML, Dalla Serra M, Menestrina G (1999) Cysteine-scanning mutagenesis of an eukaryotic pore-forming toxin from sea anemone: topology in lipid membranes. Eur J Biochem 263:128–136. doi:10.1046/j.1432-1327.1999.00477.x

Athanasiadis A, Anderluh G, Maček P, Turk D (2001) Crystal structure of the soluble form of equinatoxin II, a pore-forming toxin from the sea anemone *Actinia equina*. Structure 9:341–346. doi:10.1016/S0969-2126(01)00592-5

Belmonte G, Pederzolli C, Maček P, Menestrina G (1993) Pore formation by the sea anemone cytolysin equinatoxin II in red blood cells and model lipid membranes. J Membr Biol 131:11–22. doi:10.1007/BF02258530

Brahms S, Brahms J (1980) Determination of protein secondary structure in solution by vacuum ultraviolet circular dichroism. J Mol Biol 138:149–178. doi:10.1016/0022-2836(80)90282-X

Clarke DT, Jones GR (2004) CD12: a new high-flux beamline for ultraviolet and vacuum-ultraviolet circular dichroism on the SRS, Daresbury. J Synchrotron Radiat 11:142–149. doi:10.1107/S0909049503024142

Compton LA, Johnson WC Jr (1986) Analysis of protein circular dichroism spectra for secondary structure using a simple matrix multiplication. Anal Biochem 155:155–167. doi:10.1016/0003-2697(86)90241-1

Cornell BA, Fletcher GC, Middlehurst J, Separovic F (1981) The temperature dependence of the size of phospholipid vesicles. Biochim Biophys Acta 642:375–380. doi:10.1016/0005-2736(81)90453-3

Cornell BA, Fletcher GC, Middlehurst J, Separovic F (1982) The lower limit to the size of small sonicated phospholipid vesicles. Biochim Biophys Acta 690:15–19. doi:10.1016/0005-2736(82)90233-4

Cornell BA, Weir LE, Separovic F (1988) The effect of gramicidin A on phospholipid bilayers. Eur Biophys J 16:113–119

Drechsler A, Potrich C, Sabo JK, Frisanco M, Guella G, Dalla Serra M, Anderluh G, Separovic F, Norton RS (2006) Structure and

activity of the N-terminal region of the eukaryotic cytolysin equinatoxin II. Biochemistry 45:1818–1828. doi:10.1021/bi052166o

Filippov A, Orädd G, Lindblom G (2003) The effect of cholesterol on the lateral diffusion of phospholipids in oriented bilayers. Biophys J 84:3079–3086. doi:10.1016/S0006-3495(03)70033-2

Gutiérrez-Aguirre I, Barlič A, Podlesek Z, Maček P, Anderluh G, González-Mañas JM (2004) Membrane insertion of the N-terminal helix of equinatoxin II, a sea anemone cytolytic toxin. Biochem J 384:421–428. doi:10.1042/BJ20040601

Hinds MG, Zhang W, Anderluh G, Hansen PE, Norton RS (2002) Solution structure of the eukaryotic pore-forming cytolysin equinatoxin II: implications for pore formation. J Mol Biol 315:1219–1229. doi:10.1006/jmbi.2001.5321

Hong Q, Gutiérrez-Aguirre I, Barlič A, Malovrh P, Kristan K, Podlesek Z, Maček P, Turk D, González-Mañas J, Lakey JH, Anderluh G (2002) Two step membrane binding by equinatoxin II, a pore-forming toxin from the sea anemone, involves an exposed aromatic cluster and a flexible helix. J Biol Chem 277:41916–41924. doi:10.1074/jbc.M204625200

Kahya N, Scherfeld D, Bacia K, Poolman B, Schwille P (2003) Probing lipid mobility of raft-exhibiting model membranes by fluorescence correlation spectroscopy. J Biol Chem 278:28109–28115. doi:10.1074/jbc.M302969200

Lees JG, Smith BR, Wien F, Miles AJ, Wallace BA (2004) CDtool—an integrated software package for circular dichroism spectroscopic data processing, analysis and archiving. Anal Biochem 332:285–289. doi:10.1016/j.ab.2004.06.002

Lees JG, Miles AJ, Wien F, Wallace BA (2006) A reference database for circular dichroism spectroscopy covering fold and secondary structure space. Bioinformatics 22:1955–1962. doi:10.1093/bioinformatics/btl327

Lobley A, Whitmore L, Wallace BA (2002) DICHROWEB: an interactive website for the analysis of protein secondary structure from circular dichroism spectra. Bioinformatics 18:211–212. doi:10.1093/bioinformatics/18.1.211

Malovrh P, Viero G, Dalla Serra M, Podlesek Z, Lakey JH, Maček P, Menestrina G, Anderluh G (2003) A novel mechanism of pore formation. J Biol Chem 278:22678–22685. doi:10.1074/jbc.M300622200

Manavalan P, Johnson WC Jr (1987) Variable selection method improves the prediction of protein secondary structure from circular dichroism spectra. Anal Biochem 167:76–85. doi:10.1016/0003-2697(87)90135-7

Mao D, Wallace BA (1984) Differential light scattering and absorption flattening optical effects are minimal in the circular dichroism spectra of small unilamellar vesicles. Biochemistry 23:2667–2673. doi:10.1021/bi00307a020

Marsh D (1990) Handbook of lipid bilayers. CRC Press Inc, Boca Raton

Miles AJ, Wien F, Lees JG, Rodger A, Janes RW, Wallace BA (2003) Calibration and standardisation of synchrotron radiation circular dichroism (SRCD) amplitudes and conventional circular dichroism (CD) spectrophotometers. Spectroscopy 17:653–661

Miles AJ, Whitmore L, Wallace BA (2005) Spectral magnitude effects on the analyses of secondary structure from circular dichroism spectroscopic data. Protein Sci 14:368–374. doi:10.1110/ps.041019905

Miles AJ, Drechsler A, Kristan K, Anderluh G, Norton RS, Wallace BA, Separovic F (2008) The effects of lipids on the structure of the eukaryotic cytolysin equinatoxin II: a synchrotron radiation circular dichroism spectroscopic study. Biochim Biophys Acta 1778:2091–2096. doi:10.1016/j.bbamem.2008.04.001

Provencher SW, Glockner J (1981) Estimation of globular protein secondary structure from circular dichroism. Biochemistry 20:33–37. doi:10.1021/bi00504a006

Schön P, García-Sáez AJ, Malovrh P, Bacia B, Anderluh G, Schwille P (2008) Equinatoxin II permeabilizing activity depends on the presence of sphingomyelin and lipid phase coexistence. Biophys J 95:691–698. doi:10.1529/biophysj.108.129981

Smith R, Separovic F, Milne TJ, Whittaker A, Bennett FM, Cornell BA, Makriyannis A (1994) Structure and orientation of the pore-forming peptide, melittin, in lipid bilayers. J Mol Biol 241:456–466. doi:10.1006/jmbi.1994.1520

Sreerama N, Woody RW (1993) A self-consistent method for the analysis of protein secondary structure from circular dichroism. Anal Biochem 209:32–44. doi:10.1006/abio.1993.1079

Sreerama N, Venyaminov SY, Woody RW (1999) Estimation of the number of α-helical and β-strand segments in proteins using circular dichroism spectroscopy. Protein Sci 8:370–380

Van Stokkum IHM, Spoelder HJW, Bloemendal M, Van Grondelle R, Groen FCA (1990) Estimation of protein secondary structure and error analysis from circular dichroism spectra. Anal Biochem 191:110–118. doi:10.1016/0003-2697(90)90396-Q

Wallace BA, Lees J, Orry AJW, Lobley A, Janes RW (2003) Analyses of circular dichroism spectra of membrane proteins. Protein Sci 12:875–884. doi:10.1110/ps.0229603

Whitmore L, Wallace BA (2004) DICHROWEB, an online server for protein secondary structure analyses from circular dichroism spectroscopic data. Nucleic Acids Res 32:W668–W673

Whitmore L, Wallace BA (2008) Protein secondary structure analyses from circular dichroism spectroscopy: methods and reference databases. Biopolymers 89:392–400. doi:10.1002/bip.20853